A Time-lapse Video Image Intensification
Analysis of Cytoplasmic Organelle Movements
during Endosome Translocation

BRIAN HERMAN* and DAVID F. ALBERTINI*‡
*Department of Anatomy and ‡Laboratory of Human Reproduction and Reproductive Biology, Harvard
Medical School, Boston, Massachusetts 02115. Dr Herman's present address is Department of Anatomy,
Laboratory of Cell Biology, University of North Carolina, Chapel Hill, North Carolina 27514: Dr. Albertini's
present address is Department of Anatomy and Cellular Biology, Tufts University School of Medicine,
Boston, Massachusetts 02111.

ABSTRACT Vital fluorescence staining has been used in conjunction with time-lapse video image intensification microscopy to analyze the distribution and movement of endosomes, lysosomes, and mitochondria in cultured rat ovarian granulosa cells. Exposure of 5-d granulosa cell cultures to pyrene-concanavalin A (P-Con A) or 3,3'-dioctadecylindocarbocyanine-labeled low-density lipoprotein (dil-LDL) at 4°C results in the formation of randomly distributed endosomes 10 min after warming to 37°C that exhibit saltatory motion for 20 min. If granulosa cells are labeled at 4°C with both P-Con A and dil-LDL and warmed to 37°C, both ligands are found within the same endosomes which migrate centripetally to the cell center where label accumulates within phase-dense structures by 60 min. The initial endosome saltations occur over short distances (mean distance = 4.6 μm) with a mean velocity of 0.03 μm/s. Endosome saltations then cease and are followed by a gradual centripetal migration of endosomes to the cell center where they accumulate and fuse with phase-dense structures. The second phase of movement involves a continuous, unidirectional migration of endosomes over distances ranging from 5 to 40 μm at a mean velocity of 0.05 μm/s. Lysosomes were simultaneously visualized as acridine orange-staining, phase-dense structures in control cells and cells exposed to fluorescent ligands. In untreated cells, lysosomes are dispersed throughout the cytoplasm and undergo bidirectional saltations covering a mean distance of 8.7 μm with a mean velocity of 0.3 μm/s. Lysosomes redistribute centripetally to the perinuclear region of the cell by saltatory movement within 20 min of exposure to ligand. Mitochondria were visualized with the fluorescent dye rhodamine 123 in granulosa cells labeled with P-Con A and were found to redistribute to the cell center coincident with endosomes.

The microtubule-disrupting agent nocodazole was found to inhibit lysosome saltations and all phases of endosome movement. Taxol, a microtubule-stabilizing agent, partially impaired lysosome movement and led to a redistribution of lysosomes into linear aggregates surrounding the nucleus. Taxol was also found to inhibit endosome movement. The data indicate that (a) endosome movement proceeds initially by saltation and later by a nonsaltatory centripetal migration in association with mitochondria, that (b) lysosomes and endosomes undergo a temporally distinct but spatially similar change in cytoplasmic distribution, and that (c) microtubules are required for the directed translocation of endosomes and lysosomes towards the cell center.

Endocytosis is a constitutive cellular process used for the sequestration of both soluble and membrane-bounded materials into the cytoplasm. The first demonstration that vesicular structures mediated the uptake and transport of endocytosed material in cells was based on the classical cinemaphotography studies of Lewis made in the 1930's (28, 29). Lewis observed

that in cultured macrophages and sarcoma cells, pinocytic vesicles formed at the cell periphery and moved "more or less centrally" until "they finally reach the central part of the cell in the neighborhood of or close to the nucleus" (29). In a series of cinemaphotography and tracer experiments on macrophages, Cohn and his colleagues showed that the centripetal migration of pinocytic vesicles was associated with the appearance of vesicle contents within lysosomes in the perinuclear region of the cell (12). That structures distinct from lysosomes were responsible for the intracellular transport of endocytosed material was first clearly illustrated by Strauss in 1964 (45). He showed by double cytochemical staining that in rat kidney tubular cells, intravenously injected horseradish peroxidase first appeared in apical "phagosomes" which were separate from acid-phosphatase bearing lysosomes. By 1 h, peroxidase reaction product was found within lysosomes surrounding the nucleus. These pioneering studies established several features of the endocytic pathway in cells that may be common to both fluid-phase and receptor-mediated mechanisms. First, internalized materials are transported through the cytoplasm within a specialized structure known variously as endocytic or pinocytic vesicles, receptosomes, or endosomes (18, 21, 29, 44, 49, 51). Second, endosomes are responsible for the delivery of their contents to lysosomes (12, 19, 31, 37). Third, endosomes exhibit centripetal migration through the cytoplasm and accumulate in the cell center (12, 28, 35, 38). The characteristics of endosome translocation have not been thoroughly elucidated although there is some indication from the work of Pastan and Willingham that these structures undergo saltatory movement during their centripetal migration (35). In this respect, endosomes resemble other organelles such as lysosomes which are known to exhibit saltatory motion (16, 30, 33, 39, 50). There is, however, little direct information available on what the relationship is, if any, between the motile behavior of endosomes and the delivery of endosomal contents to lysosomes.

The objective of these experiments is to analyze the movement of endosomes in living cells with particular reference to their topographical relationship to lysosomes. Time-lapse video image intensification microscopy (TLVIM)[1] has been used in conjunction with vital fluorescence staining to examine the distribution of lysosomes and endosomes within cultured granulosa cells that have endocytosed fluorescent low-density lipoprotein (LDL) or concanavalin A (Con A). The data suggest that the interaction between endosomes and lysosomes is coordinated by discrete patterns of movement which are oriented towards the cell center.

MATERIALS AND METHODS

Cell Culture: Primary cultures of ovarian granulosa cells were established from 21-d-old immature female rats (Crl: CD Strain, Charles River Breeding Co., Wilmington, MA) primed with 17-β-estradiol (Sigma Chemical Co., St. Louis, Mo., 0.1 mg/d per animal) for 3 d prior to cell isolation. Cells were isolated as described previously (4) and plated on 22-mm square glass coverslips in Falcon 35-mm tissue culture dishes (2.0 × 10⁶ cells in 2.0 ml of medium; Falcon Labware, Div. of Becton, Dickinson & Co., Oxnard, CA). Cultures were maintained in McCoy's 5A medium supplemented with 10% donor calf serum, 100 U/ml penicillin, 5 μg/ml streptomycin sulfate, and 2.0

---

[1] *Abbreviations used in this paper.* AO, acridine orange; Con A, concanavalin A; diI-LDL, 3,3′-dioctadecylindocarbocyanine-labeled LDL; EBSSH, Earle's balanced salt solution buffered with 10 mM HEPES; F-Con A, fluoresceinated Con A; LDL, low-density lipoprotein; P-Con A, pyrene-Con A; TLVIM, time-lapse video image intensification microscopy.

mM L-glutamine at 37°C in a humidified atmosphere (95% air, 5% CO₂). All culture materials were purchased from Grand Island Biological Company, Grand Island, NY. The cells were allowed to attach and spread for 96-120 h in culture before coverslips were mounted in a perfusion chamber for video monitoring (see below). For 3,3′-dioctadecylindocarbocyanine-labeled LDL (diI-LDL) labeling experiments, 3-d-old cultures were maintained for 48 h in serum-free McCoy's 5A medium containing 2 μg/ml bovine insulin, 5 μg/ml human transferrin, and 40 ng/ml hydrocortisone (obtained from Sigma Chemical Co.).

Ligand Treatments and Vital Staining of Lysosomes and Mitochondria: Concanavalin A (Con A, Sigma Chemical Co.) was coupled to succinimidyl-1-pyrene acrylate (Molecular Probes, Junction City, OR) and purified by affinity chromatography as described previously (23). Experiments were designed as follows to simultaneously examine the distribution of pyrene-Con A (P-Con A) containing endosomes and lysosomes. 5-d granulosa cell cultures were exposed to 10 μg/ml of P-Con A for 10 min at 37°C in PBS containing Ca²⁺, Mg²⁺, and glucose at pH 7.4. The cells were rinsed three times in PBS, and coverslips were mounted into a specifically designed chamber which permitted continual observation and video recording of living cells. Acridine orange (AO), a vital stain that accumulates in lysosomes and fluoresces orange (40, 52), was infused into the chamber at a final concentration of 10 μg/ml in Earle's balanced salt solution buffered with 10 mM HEPES (EBSSH), pH 7.4. After 1 min at room temperature, EBSSH without AO was perfused into the chamber until no AO fluorescence was detectable in the effluent as determined spectrophotometrically. Approximately 2 min after exposure to AO the chamber was placed on the microscope stage maintained at 37°C with a Sage air curtain (Sage Instruments Div., Cambridge, MA), and continuous phase/fluorescence observations were made. The epiillumination system of the fluorescence microscope was adapted to permit observation of P-Con A or AO fluorophores either individually or simultaneously; both fluorophores excite at 380 nm (UG-1 excitation filter with a FL-395 dichroic mirror), whereas the emission maximum for P-Con A is 460 nm (420-nm-long pass filter), and that of AO is 650 nm (40, 52). The insertion of a 500-nm KP interference filter allows pyrene fluorescence to be observed while filtering out the AO signal; removal of this interference filter and the insertion of a 580-nm-long pass filter allows for the observation of AO fluorescence independent of the pyrene.

5-d granulosa cell cultures deprived of serum for 48 h were used to examine the distribution of LDL labeled with the fluorescent probe 3,3′-dioctadecylindocarbocyanine prepared according to the method of Pitas et al. (38). Cultures grown on glass coverslips were washed two times with EBSSH for 30 min at 4°C and labeled for 1 h at 4°C with 10 μg/ml diI-LDL in serum-free McCoy's medium. For single-label experiments, the cells were washed twice with cold EBSSH and either fixed immediately with 3.7% formaldehyde in serum-free medium for 30 min at 4°C or warmed to 37°C in serum-free medium and fixed as described above at 10, 30, or 60 min after the end of the labeling period. Double-label experiments with fluoresceinated Con A (F-Con A) were performed by labeling washed cultures for 20 min at 4°C with 10 μg/ml F-Con A either before or after labeling with diI-LDL as described above. These cultures were fixed either at 4°C or at 10, 30, or 60 min after being warmed to 37°C. The specificity of diI-LDL binding was checked by incubation of cultures in a solution of diI-LDL containing a 10-fold excess of unlabeled LDL. No cellular staining was observed under these conditions. Cultures fixed after labeling were washed twice in PBS and mounted on a drop of 50% glycerol/PBS containing 0.02% sodium azide and stored in the dark at 4°C until examined in the fluorescence microscope. Photographs were taken using the fluorescein or rhodamine filter sets under epifluorescence illumination, and negatives were printed under identical conditions for fluorescein- and 3,3′-dioctadecylindocarbocyanine (rhodamine)-labeled material. Some cultures labeled with diI-LDL were also either stained with acridine orange as described previously or mounted in the perfusion chamber used to monitor endosome movement by TLVIM.

To examine the effect of ligand addition on the distribution of mitochondria, we incubated 5-d-old granulosa cells for 30 min at 37°C with 10 μg/ml rhodamine 123 (Molecular Probes) dissolved in McCoy's 5A medium (27). The cells were rinsed three times in EBSSH, exposed to P-Con A in PBS for 10 min at 37°C, washed two times in EBSSH, and assembled into the observation chamber. Mitochondria were observed with either the fluorescein or rhodamine filter sets of the III RS vertical illuminator while P-Con A was observed as described previously.

Treatment of Granulosa Cells with Anti-Mitotic Agents: Taxol was dissolved in DMSO at a stock concentration of 10.0 mM and stored in the dark at −20°C. Nocodazole (Aldrich Chemical Co, Milwaukee, WI) was stored as a 1.0 mg/ml stock in DMSO at −20°C. Aliquots of both drugs were thawed just before dilution into fresh control culture medium. All control media contained 0.01% DMSO carrier. Fresh drug was added at a final concentration of 1.0 μM to 4-d cultures of granulosa cells which were used 24 h later for fluorescence labeling experiments with AO or rhodamine 123. Under
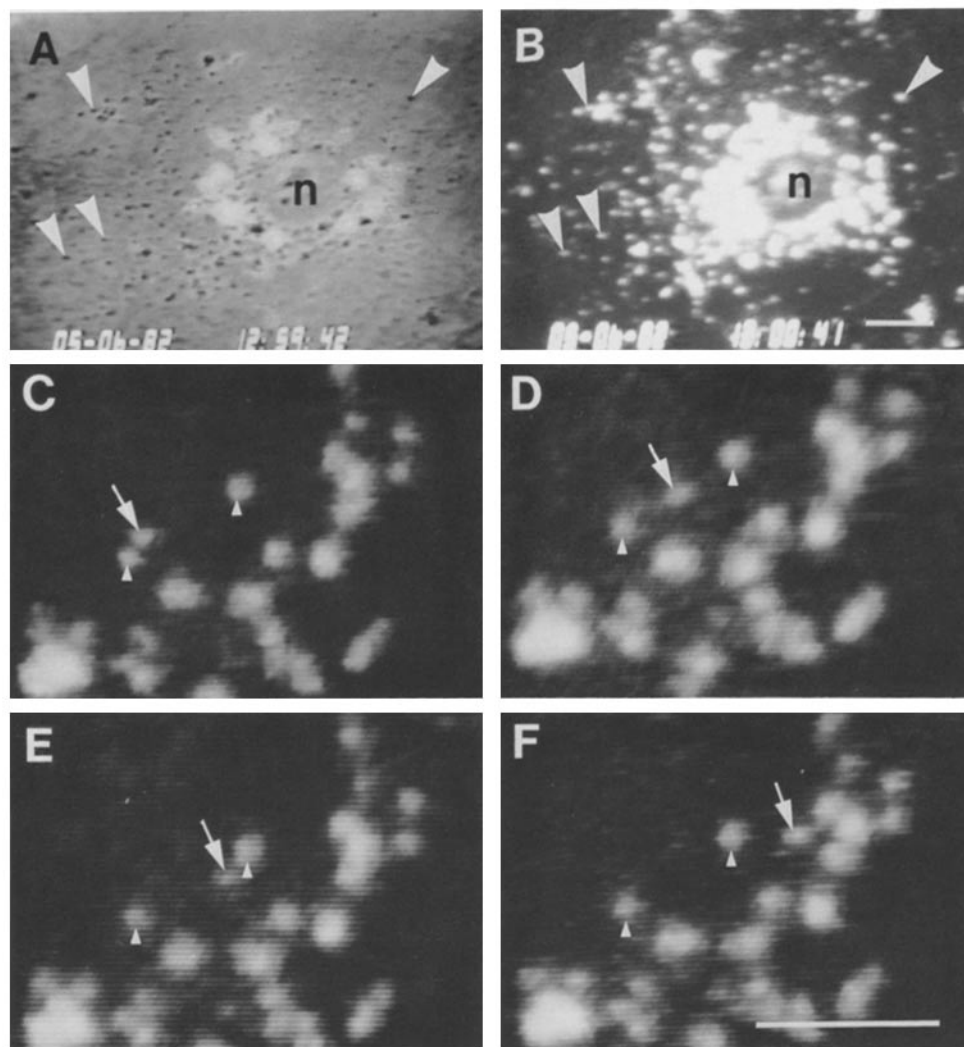
FIGURE 1 Time-lapse video images of cultured granulosa cells stained with AO to follow lysosome movement. A and B illustrate corresponding phase-contrast and fluorescent images of a control cell exhibiting a relatively dispersed population of phase-dense granules ∨ (A, ∨arrowheads) most of which are AO positive (B, arrowheads). Saltation of an individual lysosome (arrow) is shown in C-F relative to the stationary position of two nearby lysosomes (arrowheads). The total elapsed time in C-F is 33 s; n, nucleus. Bars, 10 μm.

these conditions, nocodazole has been shown to cause complete microtubule disassembly whereas taxol elicits the formation of microtubule bundles (3, 25).

Time-Lapse Video Image Intensification Microscopy (TLVIM): The system used consists of a Zeiss photoscope III equipped with a III RS vertical illuminator combining filters for the selective excitation and emission of rhodamine, fluorescein, and pyrene fluorescence as described above. Coupled to the microscope is a Venus Scientific DV-2 image intensification camera, a Panasonic NV-8030 time-lapse video tape recorder, RCA day-date-time generator, and Conrac SN/9 monitor. Cells grown on coverslips were enclosed in a chamber designed for continuous video monitoring (specifications available upon request). The chamber was machined from a piece of brass and has a 22-mm square coverslip permanently mounted to the bottom with glue. A thin film of vaseline jelly is placed under the top coverslip containing the cells, and the coverslip is inverted and secured into the chamber. A 5-ml syringe is attached to each side of the chamber with tygon tubing, and solutions are infused through one side of the chamber and withdrawn through the other. The design of the chamber allows for the addition of ligands or drugs to the cells while under continuous observation.

Photographs were obtained from single frame playback of images previously recorded on the videotape recorder off of a Conrac SN/9 television monitor utilizing a CU5 Polaroid land camera with a 5-inch lens connected to a cathode ray tube hood. Images were photographed on Polaroid type 665 positive/negative film. When image intensification was not required, micrographs were taken on Tri-X film developed with full strength Acufine at an effective ASA of 1600.

The mean distance and mean velocity of endosome or lysosome movements were analyzed by constructing two-dimensional maps of endosome and lysosome populations at various times after ligand treatment. Clear plastic overlays were attached to a 19-inch (diagonal) TV monitor through which video sequences were replayed so that the movement of individual particles could be traced (see Fig. 5, E-G); distance measurements were performed by dividing

the monitor screen into 5-μm divisions, employing a micrometer slide under the identical magnification used to examine the cells. Routinely, measurements were made from at least five randomly selected particles per cell, and at least 10 cells from three to four different sets of cultures were analyzed for a given experimental treatment or time point.

RESULTS

Lysosome Saltations in Granulosa Cells

To characterize the cytoplasmic distribution and movement of lysosomes in control granulosa cells, we perfused cultures with 10 μg/ml AO, an aniline dye commonly used to stain lysosomes (40, 52), and analyzed them by TLVIM. Corresponding phase-contrast and fluorescence micrographs indicate that >90% of the phase-dense particles observed are positively stained with AO (Fig. 1, A and B). In ~70% of the cells examined, the lysosomes are dispersed throughout the cytoplasm as discrete AO-positive spots; the remaining 30% of cells exhibit lysosomes distributed around the nucleus (Table I). The larger accessible volume in the perinuclear region of the cell results in an apparent increase in the observed fluorescence intensity (Fig. 1 B) due to the superimposition of labeled structures (47). From TLVIM analysis, the saltatory activity of lysosomes is readily apparent. The use of attenuated illumination permitted continuous observation of lysosome movement for periods of up to 10 min. As shown

in Fig. 1, C–F, the AO-staining structures exhibit rapid linear translocations towards or away from the nucleus, covering distances of ~10 μm. Although lysosomes move asynchronously within a given cell, the mean distances traversed and the mean velocities of this movement are relatively uniform between cells or within a single cell. These measurements are summarized later (Table II). Thus, the majority of the phase-dense particles observed in granulosa cells appear to be lysosomes that exhibit saltatory movement. We next analyzed the distribution of lysosomes in granulosa cells that had been exposed to Con A, a ligand which is known to be endocytosed rapidly within the coated vesicles (2, 21), or diI-LDL.

Simultaneous Observation of Lysosomes and Endosomes

The ability to simultaneously localize lysosomes and endosomes within a single living cell takes advantage of the fact that P-Con A and AO can be excited at the same wavelength (380 nm) but exhibit spectrally distinct emission maxima (pyrene acrylate, $em_{max} = 460$ nm; AO, $em_{max} = 650$ nm) that are distinguishable with appropriate filter sets. Using the filter combinations described in Materials and Methods to discriminate between the fluorescence emission of pyrene and AO, endosomes (P-Con A) and lysosomes (AO) were visualized in single intact cells at various times after P-Con A treatment to analyze their relative distributions during the centripetal migration of endosomes (21). Fig. 2 is a composite of phase-contrast and fluorescence TLVIM images demonstrating the

TABLE I

Effects of Serum, diI-LDL, and Con A on Lysosome Aggregation in Serum-deprived Cultures

Treatment	Dispersed	Aggregated
	%	
Control	79	21
Serum-free	93	7
1% serum	47	53
10% serum	27	73
10 μg/ml diI-LDL	32	68
10 μg/ml diI-LDL plus 10 μg/ml Con A	29	71

5-d cultures grown on glass coverslips and maintained in serum-free medium for 48 h were treated with McCoy's 5A medium containing serum, diI-LDL, or diI-LDL and Con A at the concentrations indicated for 30 min at 4°C, and were warmed to 37°C for 30 min before staining with AO as indicated in the Materials and Methods. 150–200 cells per coverslip were counted and scored as showing either dispersed or aggregated patterns of AO staining. The percentage of cells in each category is indicated.

temporal and spatial relationships of endosomes and lysosomes at 10 (A–C), 30 (D–F), or 60 (G–I) min after treatment with 10 μg/ml P-Con A. After a 10-min exposure to P-Con A, lysosomes exhibit a relatively random distribution throughout the cytoplasm (Fig. 2, A and C) and P-Con A labels cell surface receptors, some of which represent forming endosomes (arrows, Fig. 2B). Over the next 20 min, P-Con A is completely internalized within endosomes which are scattered throughout the cytoplasm (Fig. 2E) whereas lysosomes have reorganized and become aggregated around the nucleus (Fig. 2F). By phase-contrast microscopy it appears that some phase-dense organelles that do not bind AO remain more peripherally disposed (Fig. 2D). Endosomes containing P-Con A fuse with each other (21) and gradually accumulate around the nucleus over the next 30 min of incubation at 37°C, residing in the same region of the cell occupied by lysosomes (Fig. 2I) and most phase-dense structures (Fig. 2G). Labeling of cells with AO 30 min after endosome formation demonstrated that endosomes do not take up AO. The results indicate that exposure of granulosa cells to P-Con A induces lysosome migration to the cell center prior to the directed translocation of endosomes into the same region. It was recently shown that the rapid centripetal aggregation of lysosomes is by no means unique to Con A since a variety of ligands exerting known physiological actions on granulosa were capable of inducing this response (24). To further substantiate this effect, and to ascertain whether the structures containing Con A were equivalent to those bearing a more physiological marker for endocytosis, we performed studies with a fluorescent derivative of LDL, a prototype ligand for much of the work done on receptor-mediated endocytosis (19).

Granulosa cells deprived of serum for 48 h in culture retain their spread morphology and exhibit a predominantly dispersed population of lysosomes as determined by AO staining. A comparison of cultures maintained in the presence or absence of serum illustrates that serum deprivation increases the percentage of cells containing dispersed lysosomes (Table I). The readdition of medium containing 1 or 10% serum or 10 μg/ml diI-LDL causes an increase in the number of granulosa cells exhibiting aggregated lysosomes that is not affected by the concomitant exposure of these cells to 10 μg/ml F-Con A. Thus Con A does not modify the rapid aggregation of lysosomes induced in serum-free cultures of granulosa cells by either serum or LDL. Fluorescence microscopy of living and fixed cultures was used to follow the disposition of diI-LDL in cells labeled only with this probe or in cells labeled with both LDL and Con A.

TABLE II

Characteristics of Organelle Movement in Cultured Granulosa Cells

Organelle	Type of movement	Treatment	Mean velocity	Mean distance
			μM/sec ± SEM	μM ± SEM
Lysosome	Saltatory	None	0.30 ± 0.03	8.7 ± 0.9
	Saltatory	Taxol	0.12 ± 0.02	4.4 ± 0.4
	Brownian	Nocodazole	0.09 ± 0.01	2.2 ± 0.2
Endosome	Saltatory	None	0.03 ± 0.01	4.6 ± 0.7
	Centripetal	None	0.05 ± 0.004	36.6 ± 1.1
	—*	Taxol	—	—
	—*	Nocodazole	—	—

Estimation of organelle velocities and excursion lengths was determined from TLVIM as described in Materials and Methods, using tracings as illustrated in Fig. 5, E–G;
* Indicates that complete inhibition of movement of endosomes was observed in the presence of nocodazole or taxol (1.0 μM).
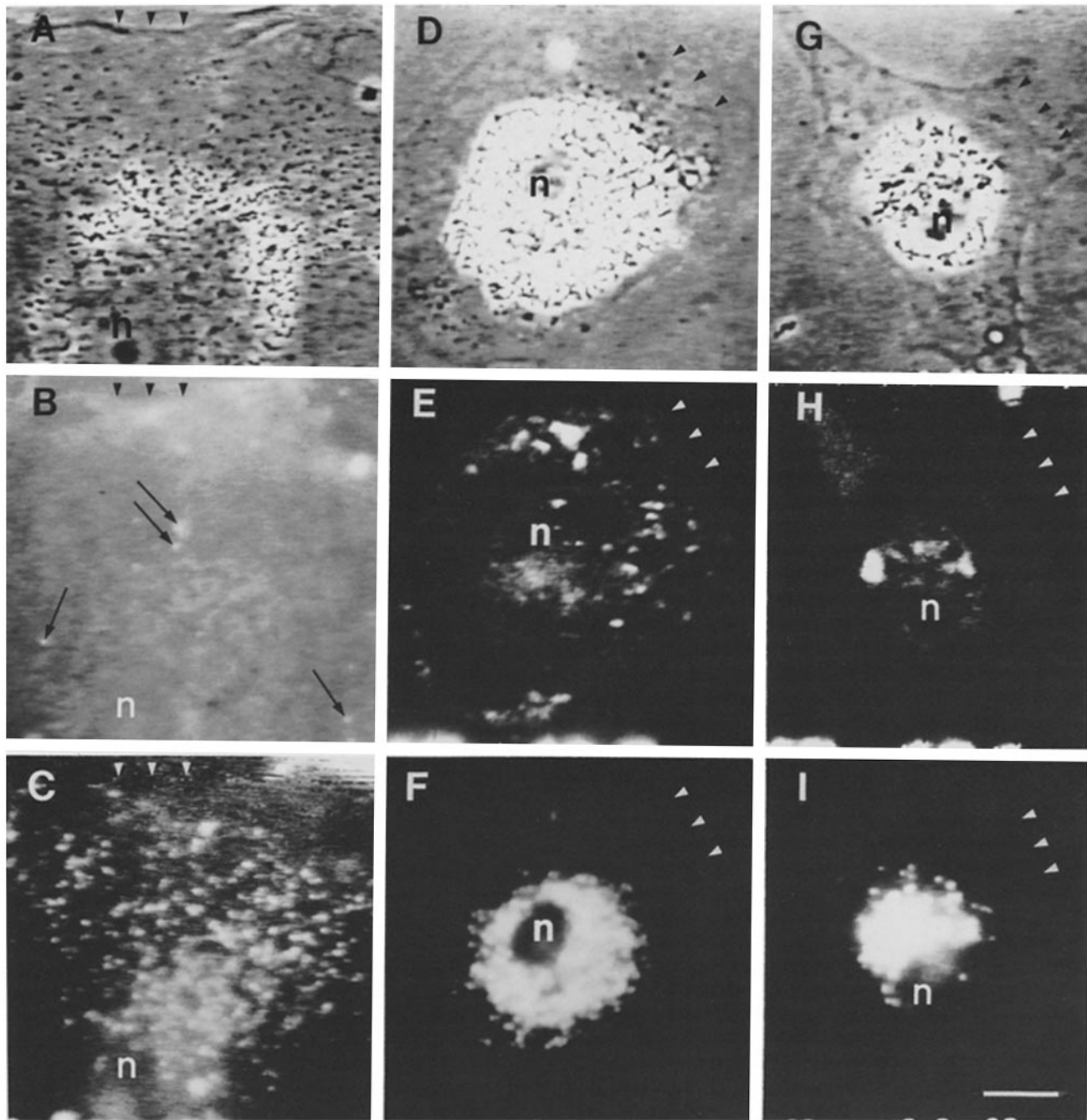
FIGURE 2 Corresponding phase-contrast (A, D, and G), P-Con A (B, E, and H), and AO (C, F, and I) micrographs of granulosa cells recorded by TLVIM various time intervals after P-Con A labeling. 10 min after labeling, phase-dense particles (A) corresponding to lysosomes (C) are distributed throughout the cytoplasm whereas P-Con A (B) labels a diffusely distributed population of cell surface receptors; newly formed endosomes are apparent by this time (arrows). By 30 min after labeling, lysosomes have reorganized around the nucleus (n, in D and F) whereas P-Con A–containing endosomes remain dispersed in the cytoplasm (E). 60 min after labeling, endosomes (H) and lysosomes (I) have accumulated at the cell center. Arrowheads demarcate the cell margins. Bar, 10 μm.

Granulosa cells from serum-free cultures fixed at 4°C after a 1-h incubation with diI-LDL at 4°C exhibit a random pattern of punctate fluorescence similar to that described in human fibroblasts (38). Warming such cultures to 37°C for as little as 15 min results in the formation of larger fluorescent spots which characteristically assume a perinuclear position by 60 min (Fig. 3A). In cultures exposed to both diI-LDL and F-Con A at 4°C and warmed to 37°C for 15 min, the distribution of both ligands is nearly identical as determined from

photomicrographs taken of the same cells under rhodamine (LDL) and fluorescein (Con A) optics (Fig. 3, B and C). In three separate experiments, it was found that ~75% of the endosomes contained both LDL and Con A and that the remaining endosomes contained only one of the ligands in equal proportions. By 60 min after warming the cells to 37°C, virtually all of the diI-LDL and F-Con A staining is confined to perinuclear endosomes of various sizes which contain both probes (Fig. 3, E and F) and reside within phase-dense struc-
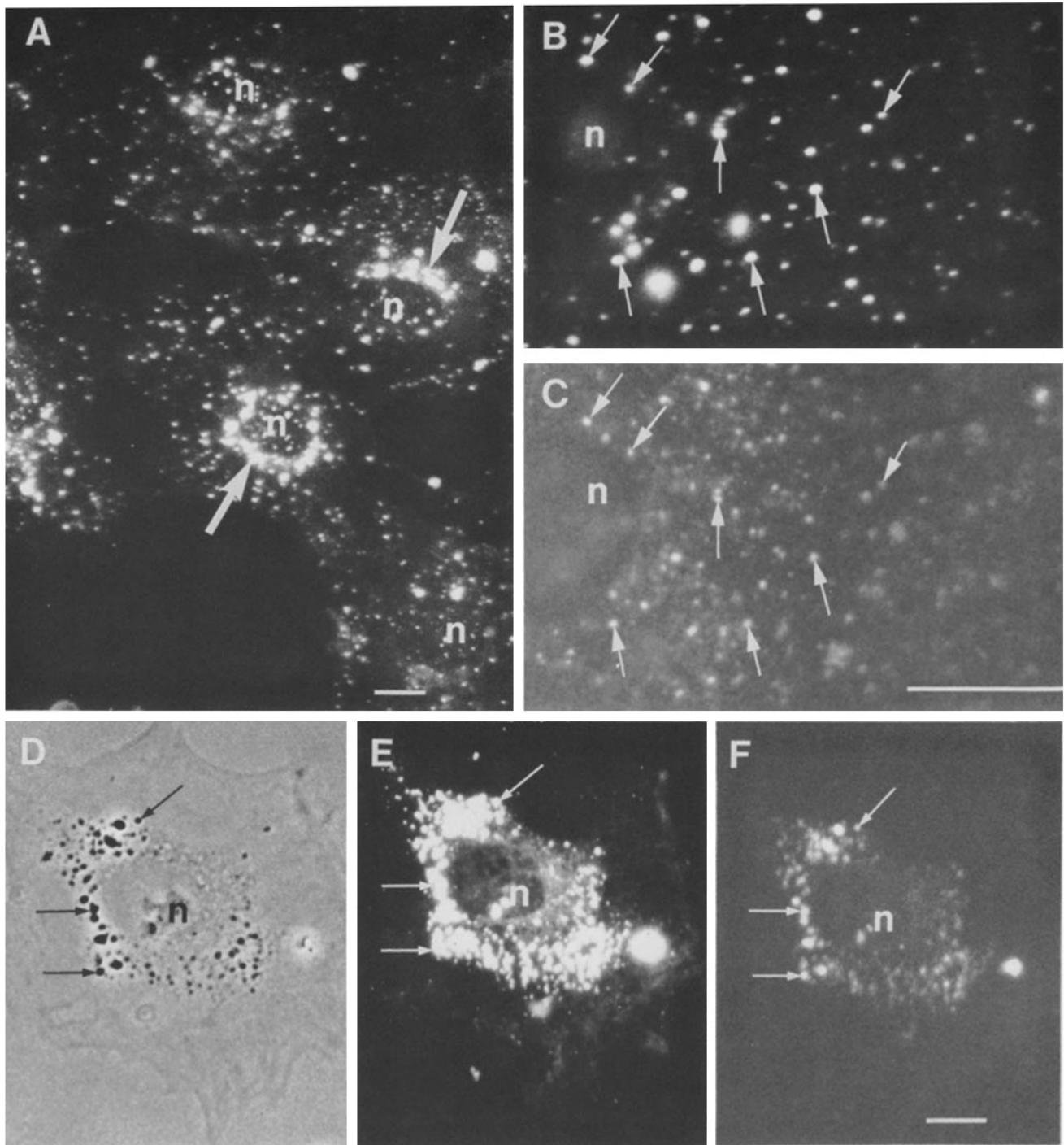
FIGURE 3   Co-distribution of diI-LDL and F-Con A within granulosa cell endosomes. *A* illustrates the punctate staining pattern of 5-d-old granulosa cell cultures fixed 15 min after labeling with diI-LDL alone as described in the Materials and Methods; note perinuclear aggregates of endosomes in the two cells marked by arrows. *B* and *C* demonstrate the corresponding diI-LDL (*B*) and F-Con A (*C*) patterns of the same granulosa cell fixed 15 min after labeling with both probes at 4°C; the arrows indicate seven endosomal structures that contain both LDL and Con A. The phase-contrast micrograph in *D* is of a granulosa cell exposed to both diI-LDL (*E*) and F-Con A (*F*) at 4°C and warmed to 37°C for 60 min before fixation; note that most of the phase-dense structures surrounding the nucleus (*n*) in *D* contain both LDL and Con A. Bars, 10 μm.

tures presumed to be lysosomes (Fig. 3*D*). Note that while all of the Con A is contained within phase-dense structures at this time, some diI-LDL–containing vesicles are present around the nucleus that are not themselves phase-dense but appear in close association with the double-labeled, phase-dense organelles. Taken together, these data illustrate that

endosomes migrate centripetally subsequent to ligand-induced lysosome aggregation and that the accumulation of these discrete organelles in the cell center is associated with the delivery of ligand to the lysosome. We next attempted to characterize the movement of endosomes and lysosomes during centripetal migration in living cells.

Patterns of Endosome and Lysosome Movement during Centripetal Translocation

The type of movement exhibited by lysosomes after P-Con A addition was examined by tracking particles that were both phase dense and stained with AO. Lysosome translocation is characterized by saltatory motion similar to that found in control cells (Fig. 1), with two exceptions. First, P-Con A treatment causes lysosomes to migrate unidirectionally towards the cell center by saltations. Second, the distances traversed by individual saltations is smaller than the mean distances travelled by lysosomes in control (DMSO) or untreated cells. The movement of endosomes was followed in cells for 10–60 min after P-Con A treatment (Fig. 4). Endosome movement occurred in two temporally distinct phases. Newly formed endosomes undergo saltatory movement during an initial phase that lasts for ~20 min after endosome

formation (Fig. 4, A–C). The mean distance of single excursions and the mean velocity of such movements is less than that observed for lysosomes within the same cell (Table I, lines 1 and 4). Saltatory motion of endosomes then ceases abruptly, at which time a steady migration of endosomes occurs directed towards the cell center. This second phase of movement is characterized initially by an inward displacement of endosomes from the cell margin. Endosomes subsequently appear to align into a crescentic wave (Fig. 4D) which gradually condenses around the nucleus (Fig. 4E) until individual endosomes become superimposed and aggregated at the cell center (Fig. 4F). Although the mean distances traversed by endosomes during this phase of movement are greater than the earlier saltatory excursions (4.6 vs. 36.0 μm), the mean velocities are quite similar (0.05 μm/s centripetal vs. 0.03 μm/s saltatory). It is interesting to note that individual endosomes situated within the crescentic wave are displaced
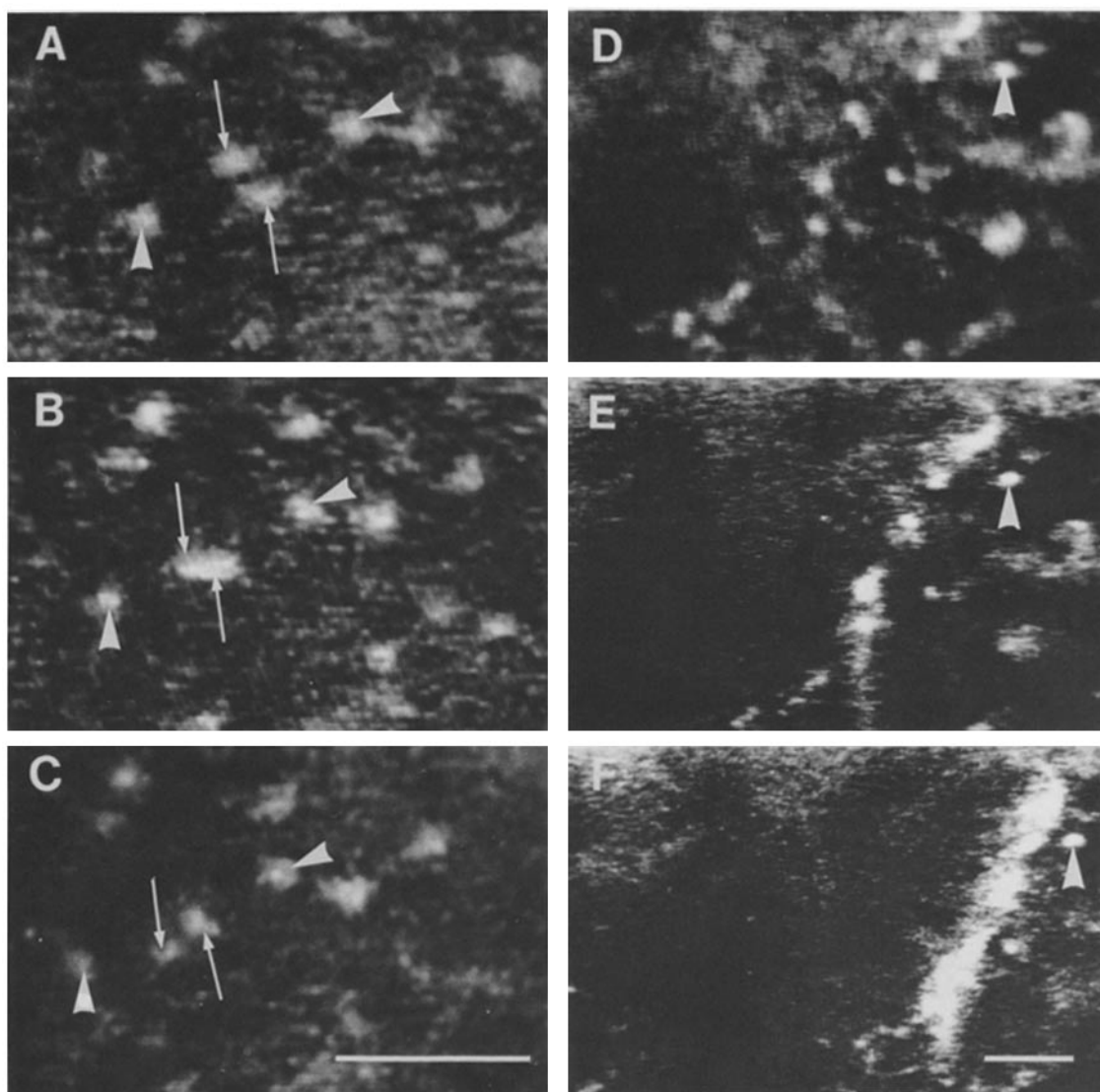

FIGURE 4 TLVIM recordings of the two phases of endosome movement. Two endosomes bearing P-Con A (arrows in A) are shown approximating each other (B) and then moving apart (C). The total elapsed time is 20 s. Saltatory motion ceases 20 min after labeling and is followed by movement of endosomes towards the nucleus (located to the right) which is depicted as endosomes align (D) and progressively migrate (E and F); note that the relative position of an endosome (arrowhead) at the leading edge of the advancing group of endosomes remains constant, suggesting a generalized displacement of endosomes to the perinuclear area from all regions of the cytoplasm. Bars, 10 μm.

centripetally as migration proceeds (Fig. 4, *C–D*, arrowheads). It is likely that the superimposition of endosomes apparent by TLVIM during migration involve endosome fusion events since previous electron microscopic studies indicate that en-

dosomes fuse and become larger during centripetal translocation (21).

Similar velocity and excursion distance measurements have been obtained in preliminary studies on diI-LDL–labeled
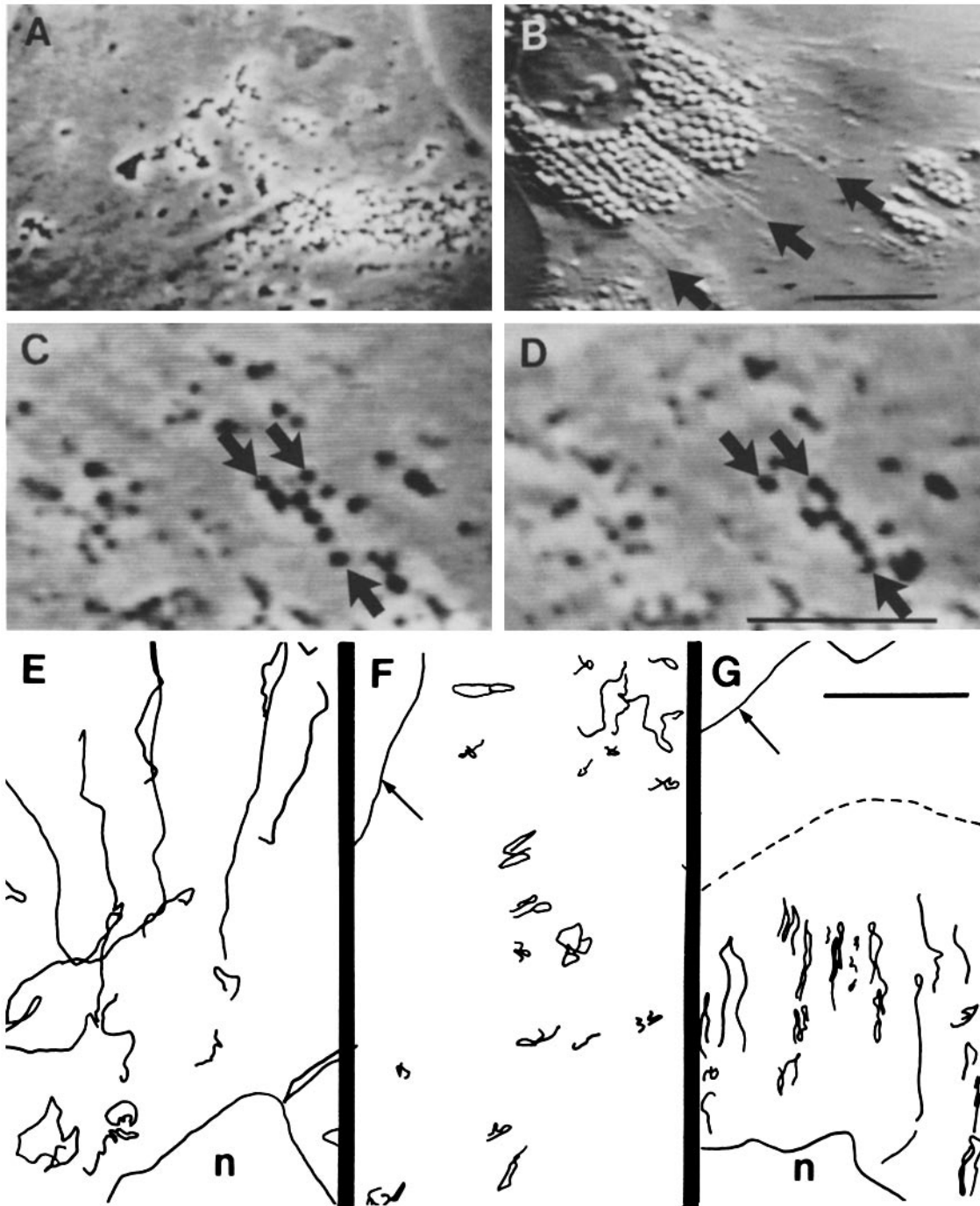

FIGURE 5   Effects of nocodazole (A) or taxol (B–D) on lysosome distribution and movement. Lysosomes aggregate in granulosa cells treated with 1.0 µM nocodazole for 24 h (A) and fail to saltate. A video-enhanced Nomarski image (obtained with an MTI-Dage 63 M camera with a Nuvicon target tube) of a granulosa cell treated with 1.0 µM taxol for 24 h is depicted in B; note the rows of organelles near the nucleus separated by straight fibrils (arrows). A time-lapse video sequence of lysosomes in a taxol-treated cell is shown in C and D; note the alignment of lysosomes in this region near the nucleus; arrows denote three sets of lysosomes that undergo repeated linear saltatory movements confined to this region of the cell. Elapsed time between C and D is 132 s. Patterns of lysosome movement are illustrated in E–G which are actual tracings of videotapes made from control (E), nocodazole-treated (F), or taxol-treated (G) granulosa cells. Long, linear excursions are characteristic of contro cells (E) whereas lysosomes in nocodazole-treated cells (F) exhibit limited local movements. In taxol-treated cells (G), lysosomes undergo short-range saltations confined to a perinuclear region indicated by the dotted line. n, nucleus; arrows indicate cell border. Bars, 10 µm.

granulosa cells in that newly formed endosomes bearing this ligand initially exhibit saltatory motion, but this activity ceases 10–15 min after warming to 37°C and is followed by a more gradual displacement towards the cell center. This pattern of movement is also reproduced in endosomes containing both Con A and LDL.

Effects of Anti-Mitotic Agents on Endosome and Lysosome Movements

The intracellular movement of cellular organelles in many, but not all, systems seems to require an intact microtubular system (8, 16, 33, 50). As demonstrated previously, endosome translocation is attended by a reorganization of microtubules and intermediate filaments (21). These findings led us to examine the influence of microtubule-perturbing agents on the cytoplasmic distribution and movement of endosomes and lysosomes. 4-d cultures of granulosa cells were exposed to either nocodazole (1.0 μM), a microtubule-depolymerizing agent (3), or taxol (1.0 μM), an agent shown to enhance assembly and stabilize microtubules in vivo (25, 41). Cells were treated with drugs for 24 h at 37°C and stained with AO, as described earlier, in solutions containing the drug at a concentration of 1.0 μM. The coverslips were mounted into the perfusion chamber in EBSSH containing drugs at appropriate concentrations. TLVIM was performed and phase-dense AO-positive particles were selected on videotape playback for the determination of the mean distance travelled, mean velocity, and movement vectors. The data are presented in Fig. 5 and Table II.

Treatment of cells with 1.0 μM nocodazole results in an inhibiton of lysosome saltations. Lysosomes form small aggregates of 5–30 particles which are situated randomly in the cytoplasm (Fig. 5A). The mean excursion distance is reduced three- to fivefold compared with untreated, or control cells (Fig. 5E and Table II, line 1) and is accompanied by a threefold reduction in the mean velocity (Table II, line 3). Video analysis showed that lysosome movement in nocodazole-treated cells is largely Brownian in character and lacks directionality since movement is confined to small areas and occurs in all directions (Fig. 5F). By contrast, taxol had quite different effects on the cytoplasmic distribution and movement of lysosomes. Under Nomarski (Fig. 5B) or fluorescence optics (not shown), lysosomes accumulated around the nucleus as groups of particles showing a marked parallel alignment along fibrous structures. Although the identity of these linear structures remains unclear, it is likely that they represent the microtubule bundles known to form in these (3, 25) and other cells (41) upon taxol treatment. The lysosomes that accumulate into perinuclear rows continue to saltate within this restricted central region of the cytoplasm. The movements are linear and bidirectional (Fig. 5, C, D, and G) and are decreased in terms of the mean distance traversed and mean velocity when compared with controls (Table II, line 2). Based on the bidirectionality and linearity of lysosome movement in taxol-treated cells, it would appear that the taxol-induced redistribution of cytoplasmic microtubules alters the pattern of saltation but does not inhibit movement itself. In contrast, nocodazole-induced disruption of microtubules alters cytoplasmic organization in a fashion that prevents normal saltations and limits movements of any kind from occurring.

The effects of these drugs on endosome movement was analyzed similarly in cells induced to form P-Con A endo-somes either shortly before (nocodazole) or after (taxol) drug treatment. As mentioned previously, endosome saltations are shorter in distance and slower in velocity than lysosome saltations (Table II, compare line 1 with line 4). Also, during their centripetal migration endosomes traverse distances ranging from 5 to 40 μm depending on their site or origin, but at velocities similar to those exhibited by endosomes during their saltatory phase of movement. Both taxol and nocodazole inhibit the movement of endosomes (Table II) which remain dispersed throughout the cytoplasm (21). When nocodazole is removed, endosomes begin to saltate within 30 min and undergo centripetal translocation to the cell center 90 min after drug removal. Much longer recovery times of 6–12 h are required to reverse the effects of taxol on endosome movement, although in contrast to nocodazole this drug has no effect on endosome formation (21). Reports that organelle movement and distribution are generally affected by microtubule-perturbing agents (14, 33) lend further support to the idea that cytoplasmic organelle disposition may be altered as a consequence of the change in cytoskeletal organization that occurs during endosome translocation in this system (21). To begin to examine this problem, we have analyzed the distribution of another cytoplasmic organelle, mitochondria, in granulosa cells exposed to P-Con A.

Effects of P-Con A on Mitochondrial Distribution

5-d cultures of granulosa cells were stained with rhodamine 123, a vital stain specifically taken up by mitochondria (27). The results are summarized in Table III with respect to the disposition of AO-stained lysosomes and rhodamine 123-stained mitochondria in granulosa cells examined at various times after Con A treatment. In control, untreated cells or cells that had been exposed to P-Con A for 10 min, mitochondria are dispersed through the cytoplasm. 30 min after exposure to P-Con A, a time corresponding to the aggregated distribution of lysosomes but a relatively dispersed distribution of endosomes, the mithchondria are retracted from the cell boundaries and, by 60 min, assume a perinuclear distribution similar to that of endosomes. The percentage of cells showing perinuclear aggregation of endosomes and mitochondria is essentially equivalent (74 vs. 68%), suggesting that these organelles undergo a concomitant redistribution. Because diI-LDL and rhodamine 123 exhibit similar fluorescence patterns, it has been difficult to resolve the disposition of mitochondria in granulosa cells bearing LDL endosomes. However, by phase-contrast microscopy (Fig. 3D) it would appear that most organelles are cleared from the peripheral

TABLE III

Time Dependence of Organelle Aggregation after P-Con A Addition

| Organelle | Distribution (% cells) | | | | | |
	D (10 min)	A (10 min)	D (30 min)	A (30 min)	D (60 min)	A (60 min)
Endosomes	—	—	84	16	26	74
Mitochondria	80	20	67	33	32	68
Lysosomes	71	29	34	66	43	57

5-d cultures were examined at various times after P-Con A addition and stained with either AO or rhodamine 123; 100–150 cells at each time point were scored with respect to organelle distribution as dispersed (D) or aggregated (A) as shown in Figs. 3 and 6. The percentage of cells in each category is indicated.

cytoplasm in cultures exposed to diI-LDL. Thus, mitochondria seem to move to the cell center in a pattern that is temporally and spatially similar to that observed for endosomes.

DISCUSSION

Among the early events associated with the endocytosis of various ligands are (a) the clustering of ligand-receptor complexes within coated pits and their retrieval by coated vesicles (6, 9), (b) the uncoating of these vesicles which fuse to form endosomes (19, 49), and (c) the acidification of endosomes which may be related to the dissociation of ligands from their receptors to allow receptor recycling (11, 17, 18, 44, 48). These events occur rapidly, within 5–10 min after warming cells to 37°C. The temporal and kinetic parameters of ligand processing during receptor-mediated endocytosis have also been well documented, and characteristically a 30–60-min lag period occurs before degraded ligand appears extracellularly (31, 34, 37). The data presented in this paper and reviewed earlier indicate that materials internalized by both fluid-phase and receptor-mediated mechanisms are transported within endosomes to the cell center during this lag period (21, 29, 35, 38, 42, 45). We have thus attempted to characterize the spatial and temporal features of endosome movement relative to lysosomes since the spatial relationship of these structures may be relevant to the intercompartmental transfer of ligands within the cytoplasm of living cells.

From a TLVIM analysis of the fate of both "opportunistic" (Con A) and physiological (LDL) ligands in ovarian granulosa cells, it was found that the translocation of endosomes to the cell center occurs in two distinct stages. The first stage of translocation, which occurs soon after ligand internalization within coated vesicles (2, 21), involves saltatory movement of endosomes. During the second stage, endosomes stop saltating and translocate centripetally to the cell center with constant velocity. The entire process is 60 min in duration and is attended by rearrangements in the distribution of both lysosomes and mitochondria. Lysosomes were found to move by saltations towards the nucleus before endosome translocation whereas mitochondria appear to redistribute during endosome translocation. Thus, the data suggest that discrete mechanisms may exist in granulosa cells for controlling the spatial distribution of certain organelles during the uptake and intracellular translocation of Con A and LDL. The generality and potential significance of these observations awaits the direct demonstration that these coordinated movements are required for ligand delivery to lysosomes. However, several lines of evidence now indicate that the segregated pattern of lysosome and endosome movement is not unique to granulosa cells.

For example, certain hormones induce a perinuclear aggregation of lysosomes in their target cells. Szego and her colleagues have shown that rat uterine endometrial cells responding to the steroid hormone estradiol (46) and rat oocytes induced to mature by luteinizing hormone (14) undergo lysosome aggregation around the nucleus shortly after hormone administration. Moreover, studies with cultured aortic smooth muscle cells indicate that serum, platelet-derived growth factor, insulin, and transferrin induce a similar change in lysosome distribution (Herman and Castellot, unpublished observation). Recent studies in granulosa cells have shown that specific hormones and extracellular matrix molecules

that influence granulosa cell function induce a similar rapid redistribution of lysosomes to the cell center upon brief exposure of cells to these ligands (24) as well as to LDL (Table I). Whether the redistribution of lysosomes induced by ligands represents a mechanism for nonrandomizing the location of lysosomes to enhance the probability of effective fusion with endosomes remains a matter of speculation although evidence is available to support this idea.

The saltatory movement of various organelles, including lysosomes, is known to be inhibited by drugs that depolymerize cytoplasmic microtubules (8, 16, 33, 39, 50). Earlier studies from this laboratory indicated that both nocodazole and taxol were effective inhibitors of endosome translocation in granulosa cells and that subpopulations of cytoplasmic microtubules and intermediate filaments reorganize during endosome translocation in this system (21). These observations are extended by the finding that nocodazole reversibly inhibited lysosome movement in granulosa cells whereas taxol, a microtubule-stabilizing agent, while not inhibiting lysosome movement, did restrict saltations to specific regions of the cytoplasm. If microtubules are responsible for facilitating and orienting organelle movements (8), then it seems likely that the efficiency of collisions between endosomes and lysosomes would be diminished, but not completely inhibited, owing to the possible random intermixing of these organelles which can occur under in vitro conditions (5). Microtubules have been shown to influence the distribution and mobility of cytoplasmic organelles (8, 16, 33, 39), and it is interesting to note that the catabolism of LDL, epidermal growth factor, and transferrin is partially inhibited by microtubule-disrupting drugs (10, 20, 34). The redistribution of mitochondria with translocating endosomes may also depend on the integrity of cytoplasmic microtubules based upon the sensitivity of organelle redistribution to microtubule-perturbing agents and the demonstration of structural interactions between mitochondria and microtubules (7, 43). A similar association of mitochondria with translocating endosomes has been noted during transferrin processing in erythropoietic cells (26). The metabolic requirements for ligand-receptor processing and organelle interactions are likely to be complex in view of the known ATP dependence of organelle movement (1, 30), the removal of clathrin from coated endosomes (36), and the acidification of endosomes and coated vesicles (17, 44). Of interest in this regard is the finding that uncouplers of oxidative phosphorylation and lysomotropic agents block the centripetal movement of endosomes and lysosomes (Albertini and Herman, unpublished observation). Further study is clearly required to establish the structural and metabolic requirements for such interactions.

Are other cytoplasmic components associated with endosomes and mitochondria as they undergo centripetal translocation? Using nitrobenzoxadial-phallicidin staining, no gross changes in the organization of F-actin containing stress fibers have been noted during endosome translocation (Herman and Albertini, unpublished observation). In addition, it is known that AO binds to ribonucleoprotein and fluoresces green under the fluorescein filter set (40); this staining remains diffuse during and after the Con A-induced redistribution of organelles. The differential sensitivity of organelle movement to certain drugs, coupled with our previous studies on the spatial relationship between microtubules and intermediate filaments with endosomes, suggests that stringent control is exerted over the selection of certain cytoplasmic components

which must coordinately reorganize during the translocation of endosomes. The cellular system and approach described in this paper seem suitable for further analysis of this problem especially in view of the response to a physiological ligand such as LDL.

The data obtained in these studies required the development of a new fluorescence microscopic technique and take advantage of certain properties of cultured granulosa cells. These cells are optically suitable for particle mapping because they (a) spread extensively, (b) form large numbers of readily identifiable endosomes, and (c) do not change shape during endosome translocation. Granulosa cells exhibit little autofluorescence which allowed for the selection and use of a range of fluorescent probes that could be discriminated from one another with appropriate filter combinations. Using attenuated illumination for TLVIM, endosomes containing either P-Con A or diI-LDL were observable for prolonged time periods without either loss of signal (photobleaching) or the inhibition of movement in cells judged to be viable by dye exclusion. It should be emphasized, however, that many of these studies rely on the use of Con A as an endosomal marker which in other systems has been shown to adversely affect such processes as proton transport (32) and endosome-lysosome fusion (13). Moreover, this approach does not permit direct observation of fusion events between endosomes and lysosomes because the broad excitation range of AO overlaps the excitation and emission range of pyrene, diI, and other commonly used fluorophores. Finally, local cell damage due to the generation of oxidative excited state species cannot be completely excluded in studies involving fluorescence staining.

In conclusion, a sequence of events during the endocytosis of Con A and LDL in cultured granulosa cells has been identified which suggests that organellar movements are subjected to precise spatial and temporal control. The generality of this behavior to other ligands in other cell types and its significance with respect to ligand processing and membrane flow in general (15) await further analysis. The notion that the coordinated organelle movements described in this paper represent a basic mechanism for enhancing the probability of functional organellar interactions required for ligand catabolism is currently under investigation.

REFERENCES

1. Adams, R. J. 1982. Organelle movement in axons depends on ATP. Nature (Lond.). 297:327–329.
2. Albertini, D. F., and J. I. Clark. 1975. Membrane-microtubule interactions: concanavalin A capping induced redistribution of cytoplasmic microtubules and colchicine binding proteins. Proc. Natl. Acad. Sci. USA. 72:4976–4980.
3. Albertini, D. F., and J. I. Clark. 1981. Visualization of assembled and disassembled microtubule protein by double label fluorescence microscopy. Cell Biology International Reports. 5:387–397.
4. Albertini, D. F., and N. K. Kravit. 1981. Isolation and biochemical characterization of ten-nanometer filaments from cultured ovarian granulosa cells. J. Biol. Chem. 256:2484–2492.

5. Altstiel, L., and D. Branton. 1983. Fusion of coated vesicles with lysosomes: measurement with a fluorescence assay. Cell. 32:921–929.
6. Anderson, R. G. W., M. S. Brown, and J. L. Goldstein. 1977. Role of the coated endocytic vesicle in the uptake of receptor-bound low density lipoprotein in human fibroblasts. Cell. 10:351–364.
7. Ball, E. H., and S. J. Singer. 1982. Mitochondria are associated with microtubules and not with intermediate filaments in cultured fibroblasts. Proc. Natl. Acad. Sci. USA. 79:123–126.
8. Beckerle, M. C., and K. R. Porter. 1983. Analysis of the role of microtubules and actin in erythrophore intracellular motility. J. Cell Biol. 96:354–362.
9. Bretscher, M. S., J. N. Thomson, and B. M. F. Pearse. 1980. Coated pits act as molecular filters. Proc. Natl. Acad. Sci. USA. 77:4156–4159.
10. Brown, K. D., M. Friedkin, and E. Rozengurt. 1980. Colchicine inhibits epidermal growth factor degradation in 3T3 cells. Proc. Natl. Acad. Sci. USA. 77:480–484.
11. Brown, M. S., R. G. W. Anderson, and J. L. Goldstein. 1983. Recycling receptors: the round-trip itinerary of migrant membrane proteins. Cell. 32:663–667.
12. Cohn, A. Z., M. E. Fedorko, and J. G. Hirsch. 1966. The in vitro differentiation of mononuclear phagocytes. V. The formation of macrophage lysosomes. J. Exp. Med. 123:757–766.
13. Edelson, P., and Z. A. Cohn. 1974. Effects of concanavalin A on mouse peritoneal macrophages. I. Stimulation of endocytic activity and inhibition of phago-lysosome formation. J. Exp. Med. 140:1364–1386.
14. Ezzell, R. M., and C. M. Szego. 1979. Luteinizing hormone-accelerated redistribution of lysosome-like organelles preceding dissolution of the nuclear envelope in rat oocytes maturing in vitro. J. Cell Biol. 82:264–277.
15. Farquhar, M. G., and G. E. Palade. 1981. The Golgi apparatus (complex) —(1954–1981)— from artifact to center stage. J. Cell Biol. 91(3, Pt. 2):77s–103s.
16. Freed, J. J., and M. M. Lebowitz. 1970. The association of a class of saltatory movements with microtubules in cultured cells. J. Cell Biol. 45:334–354.
17. Forgac, M., L. Cantley, B. Wiedenmann, L. Altstiel, and D. Branton. 1983. Clathrin-coated vesicles contain an ATP-dependent proton pump. Proc. Natl. Acad. Sci. USA. 80:1300–1303.
18. Geuze, H. J., J. W. Slot, G. J. A. M. Strous, H. F. Lodish, and A. L. Schwarz. 1983. Intracellular site of asialoglycoprotein receptor-ligand uncoupling: double-label immunoelectron microscopy during receptor-mediated endocytosis. Cell. 32:277–287.
19. Goldstein, J. L., R. G. W. Anderson, and M. S. Brown. 1979. Coated pits, coated vesicles, and receptor-mediated endocytosis. Nature (Lond.). 279:679–685.
20. Hemmaplardh, D. H., S. G. Kallis, and E. H. Morgan. 1974. The effects of inhibitors of microtubule and microfilament function on transferrin and iron uptake by rabbit reticulocytes and bone marrow. Br. J. Haematol. 28:53–65.
21. Herman, B., and D. F. Albertini. 1982. The intracellular movement of endocytic vesicles in cultured ovarian granulosa cells. Cell Motility. 2:583–597.
22. Herman, B., and D. F. Albertini. 1982. Time lapse video image intensification analysis of endosome and lysosome movements in cultured granulosa cells. J. Cell Biol. 95(2, Pt. 2):440a. (Abstr.)
23. Herman, B., and S. M. Fernandez. 1982. Fluorescent pyrene derivative of concanavalin A: preparation and spectroscopic characterization. Biochemistry. 21:3271–3275.
24. Herman, B., and D. F. Albertini. 1983. Ligand-induced rapid redistribution of lysosomes is temporally distinct from endosome translocation. Nature (Lond.). 304:739–740.
25. Herman, B., M. A. Langevin, and D. F. Albertini. 1983. The effects of taxol on the organization of the cytoskeleton in cultured ovarian granulosa cells. Eur. J. Cell Biol. 31:34–45.
26. Iacopetta, B. J., E. H. Morgan, and G. C. T. Yeoh. 1983. Receptor-mediated endocytosis of transferrin by developing erythroid cells from the fetal rat liver. J. Histochem. Cytochem. 31:336–344.
27. Johnson, L. V., M. L. Walsh, and L. B. Chen. 1980. Localization of mitochondria in living cells with rhodamine 123. Proc. Natl. Acad. Sci. USA. 77:990–994.
28. Lewis, W. H. 1931. Pinocytosis. Bulletin of the Johns Hopkins Hospital. 49:17–27.
29. Lewis, W. H. 1937. Pinocytosis by malignant cells. Am. J. Cancer. 29:666–679.
30. Luby, K. J., and K. R. Porter. 1980. The control of pigment migration in isolated erythrophores or Holocentrus ascensionis (Osbeck). I. Energy requirements. Cell. 21:13–23.
31. Merion, M., and W. S. Sly. 1983. The role of intermediate vesicles in the adsorptive endocytosis and transport of ligand to lysosomes by human fibroblasts. J. Cell Biol. 96:644–650.
32. Mikkelsen, R. B., R. Schmidt-Ullrich, and D. F. A. Wallach. 1980. Concanavalin A induces an intraluminal alkalinization of thymocyte membrane vesicles. J. Cell Physiol. 102:113–117.
33. Murphy, D., and L. Tilney. 1974. The role of microtubules in the movement of pigment granules in teleost melanophores. J. Cell Biol. 61:757–779.
34. Ostlund, R. E., B. Pfleger, and G. Schonfeld. 1979. Role of microtubules in low density lipoprotein processing by cultured cells. J. Clin. Invest. 63:75–84.
35. Pastan, I. H., and M. C. Willingham. 1981. Journey to the center of the cell: role of the receptosome. Science (Wash. DC). 214:504–509.
36. Patzer, E. J., D. M. Schlossman, and J. E. Rothman. 1982. Release of clathrin from coated vesicles dependent upon a nucleoside triphosphate and a cytosol fraction. J. Cell Biol. 93:230–236.
37. Pilch, P. F., M. A. Shia, R. J. Benson, and R. E. Fine. 1983. Coated vesicles participate in the receptor-mediated endocytosis of insulin. J. Cell Biol. 96:133–138.
38. Pitas, R. E., T. L. Innerarity, J. N. Weinstein, and R. W. Mahley. 1981. Acetoacetylated lipoproteins used to distinguish fibroblasts from macrophages in vitro by fluorescence microscopy. Arteriosclerosis. 1:177–185.
39. Rebhun, L. I. 1972. Polarized intracellular particle transport: saltatory movements and cytoplasmic streaming. Int. Rev. Cytol. 93–137.
40. Robbins, E., P. Marcus, and N. K. Gonatas. 1964. Dynamics of acridine orange-cell interaction. II. Dye-induced ultrastructural changes in multivesicular bodies (acridine orange particles). J. Cell Biol. 21:49–62.
41. Schiff, P. B., and S. B. Horwitz. 1980. Taxol stabilizes microtubules in mouse fibroblast cells. Proc. Natl. Acad. Sci. USA. 77:1561–1565.
42. Schlessinger, J., Y. Schechter, M. C. Willingham, and I. Pastan. 1978. Direct visualization of binding, aggregation, and internalization of insulin and epidermal growth factor on living fibroblastic cells. Proc. Natl. Acad. Sci. USA. 75:2659–2663.
43. Smith, D. S., U. Tarlfors, and M. L. Cayer. 1977. Structural cross-bridges between microtubules and mitochondria in central axons of an insect (Periplaneta americana). J. Cell Sci. 27:255–272.
44. Steinman, R. M., I. S. Mellman, W. A. Muller, and Z. A. Cohn. 1983. Endocytosis and the recycling of plasma membrane. J. Cell Biol. 96:1–27.
45. Strauss, W. 1964. Cytochemical observations on the relationship between lysosomes

and phagosomes in kidney and liver by combined staining for acid phosphatase and intravenously injected horseradish peroxidase. *J. Cell Biol.* 20:497–507.

46. Szego, C. M., and B. J. Seeler. 1973. Hormone-induced activation of target-specific lysosomes: acute translocation to the nucleus after administration. *J. Endocrinol.* 56:347–360.

47. Taylor, D.L., and Y.-L. Wang. 1980. Fluorescently labeled molecules as probes of the structure and function of living cells. *Nature (Lond.).* 284:405–510.

48. Tycko, B., and F. R. Maxfield. 1982. Rapid acidification of endocytic vesicles containing α₂-macroglobulin. *Cell.* 28:643–651.

49. Wall, D. A., G. Wilson, and A. L. Hubbard. 1980. The galactose-specific recognition system of the mammalian liver: the route of ligand internalization in rat hepatocytes. *Cell.* 21:79–93.

50. Wang, E., and R. D. Goldman. 1978. Functions of cytoplasmic fibers in intracellular movements in BHK-21 cells. *J. Cell Biol.* 79:708–726.

51. Willingham, M. C., and I. H. Pastan. 1980. The receptosome: an intermediate organelle of receptor-mediated endocytosis in cultured fibroblasts. *Cell.* 21:67–77.

52. Zelenin, A. V. 1966. Fluorescence microscopy of lysosomes and related structures in living cells. *Nature (Lond.).* 212:425–426.